Available online at www.sciencedirect.com
SCIENCE DIRECT®
Neuropharmacology 48 (2005) 118–133
NEURO PHARMACOLOGY
www.elsevier.com/locate/neuropharm

Cholinergic modulation of the spatiotemporal pattern of hippocampal activity in vitro

Edward O. Mann[a,b,*], Takashi Tominaga[b], Michinori Ichikawa[b], Susan A. Greenfield[a]

[a]*Department of Pharmacology, Oxford University, Mansfield Road, Oxford OX1 3QT, UK*
[b]*Laboratory for Brain-Operative Devices, Brain Science Institute, RIKEN, Hirosawa 2-1, Wako, Saitama 351-0198, Japan*

Received 16 February 2004; received in revised form 14 June 2004; accepted 17 August 2004

Abstract

The aim of this study was to use optical imaging with voltage-sensitive dyes (Di-4-ANEPPS), to examine the cholinergic modulation of CA1 network responses to Schaffer collateral input. By comparing responses recorded with optical imaging and field recordings across the proximodistal axis of CA1, it was initially demonstrated that voltage-sensitive dyes could report reliably both the pattern of activation and cholinergic modulation. The higher spatial resolution of optical imaging was used to explore the somatodendritic profile of cholinergic modulation. It was found that activation of muscarinic acetylcholine receptors (mAChR) (1–10 μM carbachol), inhibited evoked responses across all layers of CA1. This was accompanied by an increase in paired-pulse facilitation in the apical and distal dendritic layers (40 ms inter-stimulus interval), but not in perisomatic regions. The mAChR antagonist, 20 μM atropine, alone increased facilitation at perisomatic sites, suggesting that muscarinic signalling pathways actively suppress perisomatic responses to repetitive stimulation. In contrast, the activation of nicotinic acetylcholine receptors (10 μM nicotine) had no significant effect on single evoked responses, but selectively increased facilitation at perisomatic sites. These results suggest that cholinergic modulation of the hippocampal CA1 network has multiple differential effects on the somatodendritic processing of the Schaffer collateral input.

Keywords: Hippocampus; Cholinergic; Voltage-sensitive dye; Imaging

1. Introduction

The hippocampus receives a dense cholinergic projection from the medial septum/diagonal band of Broca, which plays an important role in modulating functions of learning and memory (Squire, 1992; Dutar et al., 1995). The cholinergic innervation of the hippocampus is diffuse, with few synaptic specialisations, and it is thought that acetylcholine (ACh) released in the hippocampus predominantly acts by diffuse transmission (Descarries et al., 1997). This situation implies that each ACh release site has multiple targets, capable of producing a range of heterogeneous responses in hippocampal pyramidal cells (Benson et al., 1988; Colino and Halliwell, 1993) and interneurons (Freund and Buzsaki, 1996; McQuiston and Madison, 1999c). Indeed, in addition to complexities arising from the selective pre- and post-'synaptic' distribution of various subtypes of acetylcholine receptors (AChR), it is possible for the same cholinergic agonist to produce opposite responses in the same cell type (McQuiston and Madison, 1999a). Therefore, the role of the cholinergic input to the hippocampus can only be fully understood

* Corresponding author. Department of Pharmacology, Oxford University, Mansfield Road, Oxford OX1 3QT, UK. Tel.: +44 1865 271624; fax: +44 1865 271853.
E-mail address: ed.mann@pharm.ox.ac.uk (E.O. Mann).

0028-3908/$ - see front matter © 2004 Elsevier Ltd. All rights reserved.
doi:10.1016/j.neuropharm.2004.08.022

by examining the emergent effects on the dynamics of population activity.

The cholinergic modulation of hippocampal network activity has been studied extensively using intracellular and extracellular electrophysiological recording techniques, which have provided invaluable insights into the functions of cholinergic transmission. However, the resolution of these electrophysiological recordings is spatially restricted, and may not indicate the intricate spatial patterning of neuronal activity that could be crucial to network function. For example, if a single extracellular electrode is used to monitor the cholinergic modulation of the population response to afferent stimulation, there is no information as to whether the cholinergic modulation varies across the pyramidal cell somatodendritic axis and/or varies across the extent of that hippocampal sub-region. It is possible to explore such spatial aspects of activity by imaging the changes in intrinsic reflectance or the signals from tissue bulk-loaded with Ca^{2+}-sensitive dyes (Peterlin et al., 2000), but these techniques have a poor temporal resolution which does not represent the underlying electrical activity. Indeed, a more direct means to explore the spatiotemporal dynamics of neuronal activity is to employ optical imaging with voltage-sensitive dyes (VSD). The potential benefits of using optical imaging with VSD in exploring hippocampal activity have long been recognized (Grinvald et al., 1982), but it is only with recent technical developments that it has become an accepted tool for studying neuronal activity, offering a unique combination of high temporal and spatial resolution (Shoham et al., 1999; Fitzpatrick, 2000; Tominaga et al., 2000).

The aim of this study was to combine extracellular field recordings with optical imaging with VSD to explore the cholinergic spatiotemporal modulation of activity and plasticity in the Schaffer collateral input to the hippocampal CA1 network. Such a combination of electrophysiology and imaging should provide a fuller characterisation of the cholinergic modulation of CA1 network behaviour, and provide insights as to what extent such modulation can be considered homogeneous along the CA1 proximodistal (direction of CA3 to subiculum) and somatodendritic axes. Cholinergic modulation was explored by examining the effects of bath application of the muscarinic AChR (mAChR) and nicotine AChR (nAChR) agonists and anti-cholinesterases on hippocampal activity and plasticity in vitro. The bath application of cholinergic drugs used here, was not designed to mimic fast cholinergic transmission in the hippocampus, but rather to explore the roles of diffuse cholinergic transmission (Descarries et al., 1997), which might also be relevant to the mechanisms involved in the chronic cholinergic-based treatments of Alzheimer's Disease (AD) (Giacobini, 1998; Francis et al., 1999).

2. Materials and methods

2.1. Slice preparation and staining with VSD

Male rats (4–5 weeks) were anaesthetised with ether, decapitated and the brain removed. The brains were quickly cooled in ice-cold oxygenated artificial cerebrospinal fluid (ACSF), which contained, in mM: 124 NaCl, 26 $NaHCO_3$, 10 glucose, 2.5 KCl, 2 $CaCl_2$, 2 $MgSO_4$, 1.25 NaH_2PO_4, saturated with 95% O_2/5% CO_2 (pH 7.2). After cooling for 5 min, the hippocampus was dissected out along with the surrounding cortex. The blood vessels were removed, and the entire hippocampal structure was laid out on an agar block. A perpendicular cut was made through the ventral hippocampus, and this face was mounted onto a Vibroslice (752M Vibroslice, Campden Instruments Ltd) with cyanoacrylate glue. Transverse sections (400 μm) containing the hippocampus were cut and transferred to a holding chamber, consisting of a nylon mesh submerged in ACSF at 32 °C. After 10 min, slices were then transferred onto a fine-mesh filter paper (JHWP01300, Millipore) held in place by a thin plexiglass ring (15 mm o.d., 11 mm i.d. and 2 mm thick). Once mounted on the filter paper, the slices were transferred to an interface chamber, whose atmosphere was maintained by 95% O_2/5% CO_2 continuously bubbled through ACSF. The temperature of the chamber was held at 36 °C for 1 h and then constantly at room temperature. After 1 h incubation, each slice was stained for 25 min with 100 μl of the VSD solution, containing 0.2 mM Di-4-ANEPPS (Molecular Probes) in 2.5% ethanol, 0.13% Cremaphor EL (Sigma), 1.17% distilled water, 48.1% fetal bovine serum (Sigma) and 48.1% ACSF. Slices were left to recover for a further hour prior to recording (for further details see Tominaga et al., 2000).

2.2. Stimulation and electrophysiological recordings

For experiments, the slices were transferred to a fully submerged recording chamber using the plexiglass ring, and continuously perfused with ACSF at 31–33 °C, at a rate of 1 ml/min. As the slices were attached to the membrane filter, there was no need for an anchoring mesh or wire, which could have interfered with the optical recording. Glass electrodes filled with ACSF were used for both monopolar stimulation and extracellular field recording. The Schaffer collateral/commissural fibres were stimulated using a paired-pulse paradigm with an inter-stimulus interval of 40 ms, with paired-pulses delivered at 0.05 Hz. Recordings of the field excitatory postsynaptic potential (fEPSP) were made in the stratum radiatum at distal sites to the stimulation electrode, although commonly responses were also monitored at proximal sites. The stimulus strength (0.4–0.8 mA) was adjusted to evoke a half-maximal response of the initial fEPSP at the distal field

electrode. Drugs were not applied to the perfusate until the electrophysiological recordings were stable at both electrodes for a period of 20 min. Once applied, the effect of the drug was allowed to stabilise for a period of 30 min, before LTP was induced with 100 Hz tetanus for 1 s. The recording continued for at least 1 h following LTP induction. In experiments using receptor antagonists, these antagonists were applied for a period of 20 min before agonist application, thereby giving a period of 50 min between the end of the pre-drug period and LTP induction. Once applied, drugs were included in the perfusate for the rest of the experiment.

2.3. Optical recording with voltage-sensitive dye signals

The epifluorescence optics were constructed in a tandem-lens configuration (Ratzlaff and Grinvald, 1991), with 35-mm camera lens ($f = 50$ mm, F/1.4, Nikon) as the objective lens, and the objective lens of a binocular microscope ($f = 55$ mm, $\times 1.0$ for Leica MZ-APO) as the projection lens. The final magnification of the system was $\times 1.5$. The excitation light was provided by a halogen lamp source (150 W; MHF-G150LR, Moritex Corp.) passed through an excitation filter ($\lambda = 530 \pm 10$ nm) and reflected onto the specimen by a dichroic mirror. The fluorescence was passed through an absorption filter ($\lambda > 590$ nm) and projected onto the $2\,\text{mm} \times 3\,\text{mm}$ CCD sensor of the optical imaging system (MiCAM01, BrainVision). After binning, this set-up provided optical imaging with a spatial resolution of approximately 22×22 μm (Tominaga et al., 2000).

Electrophysiological recordings were used to check that the evoked responses of the slice remained stable for a period of at least 10 min before using the imaging technique. When the optical recording system was triggered, an electronically controlled shutter was opened 200 ms prior to the start of recording to avoid mechanical disturbance and rapid bleaching of the VSD. To provide an optical baseline measurement, image acquisition started 70 ms prior to stimulation. The ratio of the fractional change in fluorescence of the VSD to the initial, pre-stimulation amount of fluorescence ($\Delta F/F$) was calculated and used as the optical signal. A depolarisation produced a reduction in fluorescence of Di-4-ANEPPS, but the polarity of this signal was reversed to match the change in membrane potential.

Due to the possible problems of photo-toxicity and photo-bleaching (Zochowski et al., 2000), optical recordings were not made continuously throughout the experiment. Instead, a series of 16 optical recordings were taken for each experimental condition – control period, during drug application, and ~1 h after LTP induction. Each optical recording was acquired at a rate of 0.7 ms frame^{-1} for 341 frames. To improve the signal-to-noise ratio, the 16 optical responses were averaged together, and passed through a 5×5 (pixels in the image plane) $\times 3$ (time frames) Gaussian 3D-matrix software filter. An optical recording was also acquired for the period of tetanus stimulation for LTP induction. Each of these tetanus optical recordings was acquired at a rate of 5 ms frame^{-1} for 682 frames, and filtered as above. For these one-off optical recordings, it was clearly not possible to increase the S/N ratio through averaging. However, due to the size of the optical signal and the reduction in acquisition rate, the S/N ratio was sufficiently high with a single recording.

2.4. Imaging analysis

A typical optical signal recorded across the entire hippocampal CA1 region in response to paired-pulse stimulation is shown in Fig. 1A and B. For quantitative analysis, it was necessary to calculate certain parameters of the optical signal. Each pixel of the image window provided an optical trace of $\Delta F/F$ over time, from which the peak responses to the first and second stimulation were calculated (Fig. 1C). The paired-pulse facilitation was calculated as the peak amplitude of the second response relative to the first. Only the measures of the peak response to the first pulse and paired-pulse facilitation were used for further analysis, as is standard with electrophysiological data (Yun et al., 2000).

Due to minor differences in the shape of individual slices, the positioning of the imaging window and placement of the stimulation electrode, it was not possible to directly compare optical imaging data across different experiments. Therefore, to enable statistical analysis, the optical signals recorded across the slice were sampled using a 3×20 grid. The initial 3 points of the grid were centred on the peak response in the stratum radiatum next to stimulation electrode, and the anatomical position of the stratum pyramidale and the peak response in the stratum oriens which occurred in the same vertical plane. For these profiles, the stratum lacunosum-moleculare was not analysed, as it receives a direct projection from the entorhinal cortex, rather than the Schaffer collateral/commissural pathway (Dvorak-Carbone and Schuman, 1999). Samples were taken from each layer after every 3 pixels (~66 μm) across the CA1, with the relative vertical position of the points remaining constant, but the exact vertical position distorted to fit the contour of the stratum pyramidale.

The amplitude of the optical signal recorded depends on factors such as the loading of the dye into neuronal membranes, the area of stained membrane within each pixel and the resting membrane potential. Therefore, measures of the peak response were normalised for the primary statistical analysis, with the response in the drug application period normalised to the pre-drug period and the optical measure of LTP normalised to the response in the drug application period. This normalisation procedure was not necessary for

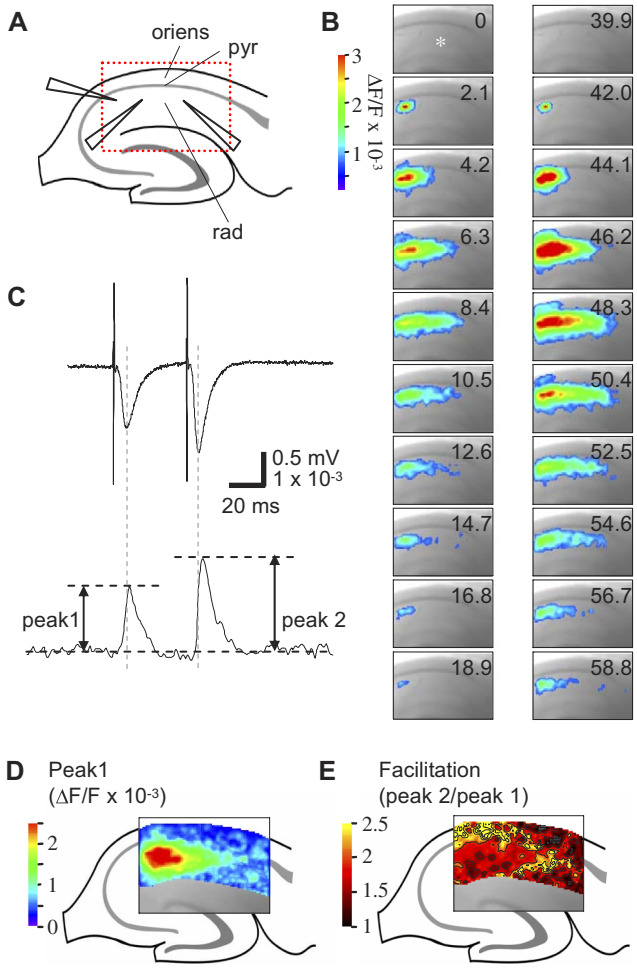

Fig. 1. Response to paired-pulse stimulation in the hippocampal CA1, recorded using optical imaging with voltage-sensitive dyes. (A) Positioning of the stimulation electrode and recording electrodes in the CA1 of the hippocampal slice. The dotted red rectangle depicts the imaging area (oriens, stratum oriens; pyr, stratum pyramidale; rad, stratum radiatum). (B) Pseudo-colour representation of the voltage changes in hippocampal CA1 in response to paired-pulse stimulation of the Schaffer collateral/commissural pathway, monitored using optical imaging with VSDs. Image acquisition was at a rate of 0.7 ms frame^{-1}, but only every 3rd frame is shown (each frame contains time in ms from first stimulation). (C) Comparison of field recording with optical recording from one pixel (shown by white star in B). The dotted vertical lines are aligned with the negative peaks in the fEPSP, showing that this coincides with the maximal change in the VSD signal. Arrows show the measurements of peak1 and peak2, used in the calculation of figures (D) and (E). (D) Pseudo-colour representation of the spatial extent of activation reached following the first stimulation pulse (peak1) across the entire CA1 region of a single hippocampal slice. (E) Pseudo-colour representation of the variation of paired-pulse facilitation of the optical response (peak2/peak1) across the entire CA1 region of the same slice depicted in (D). A floor value of 1.0 is imposed for pseudo-colour representation.

comparisons of paired-pulse facilitation, as the calculation of this parameter already entailed standardisation to the individual pattern of responses in each slice.

For more detailed analysis of the effects of cholinergic drugs on the pattern of activity across the somatodendritic axis of CA1, average optical traces were taken from the stratum oriens, stratum pyramidale, two depths of the stratum radiatum and the stratum lacunosum-moleculare. Average traces were calculated from 7×3 pixel windows at a distance from the stimulation electrode at which the optical signal in the stratum radiatum had reached 75–80% of the maximum signal. Both raw and normalised traces were calculated.

2.5. Statistical analysis

Analysis of the electrophysiological data yielded a measure of both the slope of the fEPSP for the first stimulation and paired-pulse facilitation. For statistical analysis, the electrophysiological data were pooled, giving the average of the first 20 min as the 'pre-drug' value, the average over the 10 min prior to tetanization as the 'drug application' value, and the average for a 10 min period 1 h post-tetanus as the 'LTP' value. As was the case for the imaging data, the slope of the fEPSP was normalised, with the 'drug application' value normalised to that in the 'pre-drug' period and the 'LTP' measure normalised to the 'drug application' value. Electrophysiological data were analysed in SPSS using univariate analysis of variance for 'electrode position' and 'drug treatment' (two-way ANOVA). If there was a significant effect of 'drug treatment', a post-hoc Tukey's HSD test was used to evaluate the difference between specific means.

Optical imaging data were analysed using a general linear model (GLM) repeated measures analysis of variance (RM ANOVA), performed in SPSS (SPSS inc.). Prior to analysis of variance, Mauchy's test of sphericity was used to test the assumption that the data were sampled from a multivariate normal distribution. If this assumption was violated, the degrees of freedom for tests of the within-subject effects were adjusted using the Huynh-Feldt Epsilon correction. If there was a significant between-subjects effect, a post-hoc 'Tukey's honestly significant difference test' (Tukey's HSD) was used to evaluate the difference between specific groups. If there was a significant interaction between factors, this interaction was further analysed by calculating the simple main effects, and the Sidak post-hoc pairwise multiple comparison test was used to evaluate the difference between specific factors.

2.6. Drugs and solutions

Carbachol, atropine, nicotine, mecamylamine, α-bungarotoxin, BW284c51 and tacrine were all obtained from Sigma–Aldrich Company Ltd. (Poole, UK). All drug stock solutions ($\times$ 1000) were made in distilled water, and then aliquoted and frozen at −20 °C and diluted in oxygenated ACSF immediately prior to use.

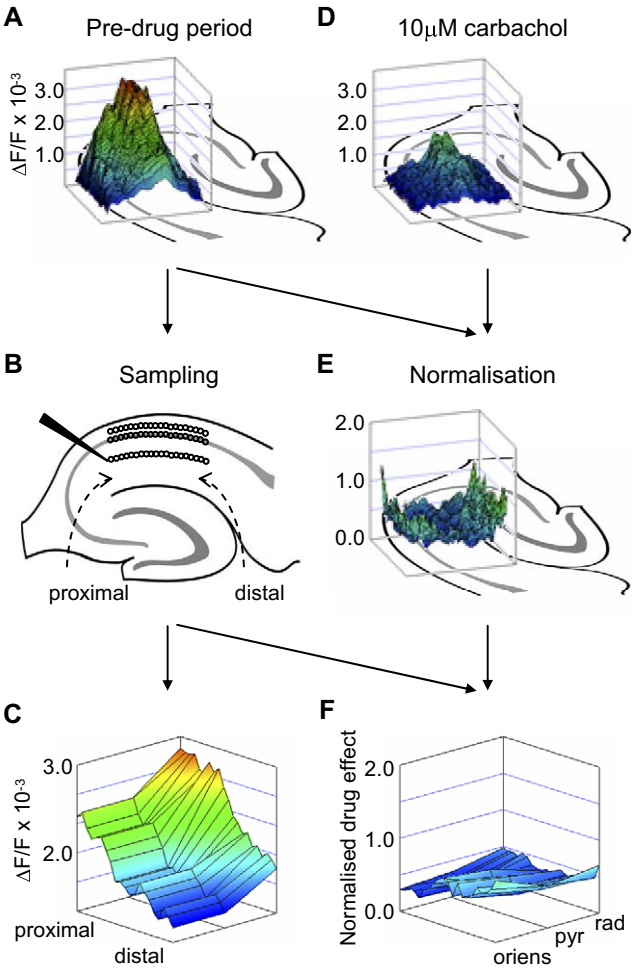

Fig. 2. Sampling and normalisation of the optical signal for statistical analysis. (A) Pseudo-colour representation of the spatial pattern of maximum response to a single stimulus in a single slice, recorded prior to application of drugs. (B) For comparisons across slices, the optical measurements were sampled with a 3×20 grid, distorted to fit the contour of the stratum pyramidale. (C) Pseudo-colour 3D graph of the sampled image from (A), with a series of 20 measurements in each stratum of CA1. (D) Pseudo-colour representation of the spatial pattern of activation to a single stimulus following application of 10 μM carbachol to the slice shown in (A). (E) Pseudo-colour representation of the normalised effect of 10 μM carbachol on a single slice. (F) Average normalised effect of 10 μM carbachol ($n = 6$), which can only be calculated following sampling. Arrows represent a flow chart of the analysis procedures (oriens, stratum oriens; pyr, stratum pyramidale; rad, stratum radiatum).

3. Results

3.1. The pattern of optical responses in the CA1 of the hippocampus

Stimulation of the Schaffer collateral/commissural pathway produced an optical signal that spread from the site of stimulation across the stratum radiatum, with a delayed signal in the stratum pyramidale and stratum oriens (Fig. 1A and B). The time course of the optical signal in the stratum radiatum was similar to that observed with electrophysiological field recordings (see Fig. 1C), with a slight delay in the optical signal. Indeed, the peak in the extracellular current coincided with the maximum change in the optical signal, consistent with the optical signal primarily reflecting voltage changes due to synaptic activation. In contrast, the optical signal in the stratum pyramidale and stratum oriens appeared to have additional components relating to action potential discharge, which were confined to regions proximal to the stimulation site (see Fig. 1B). This pattern of optical responses is consistent with that previously observed in the same preparation (Tominaga et al., 2000).

In response to paired-pulse stimulation, with an inter-stimulus interval of 40 ms, there was a facilitated response to the second stimulus observed in both the optical and electrophysiological recordings (Fig. 1C–E). The degree of paired-pulse facilitation of the fEPSP was larger than that of the optical response recorded in the same region, but as the electrophysiological field recordings measure extracellular currents and optical imaging with VSDs measure changes in membrane voltage, an exact correspondence is not expected. However, the two techniques probably reflect the same underlying physiological process, and the optical imaging allowed insight into the spatial pattern of paired-pulse facilitation. One typical feature in the pattern of paired-pulse facilitation of the optical response was a peak in the stratum pyramidale and stratum oriens proximal to the stimulation site, which was most likely due to a large increase in the number of action potentials elicited in this region by the second stimulus (see Fig. 1E). Another prominent feature was the peak in paired-pulse facilitation around the perimeter of the spatial extent of activation in response to the first stimulus (compare Fig. 1D and E). The precise location of this region was variable between slices, and presumably reflected an area where there was a low probability of initial release but a large decrease in failure rate with paired-pulse stimulation.

3.2. Quantification of the optical signal

In order to explore the effects of cholinergic drugs on the spatiotemporal pattern of activity in the hippocampal CA1, combined electrophysiological and optical imaging recordings were taken from 72 transverse hippocampal slices. As is common in the analysis of field recordings, fEPSPs were normalised to a baseline period, allowing the quantitative analysis of relative drug effects. To enable a comparison between electrophysiological and imaging techniques, while still utilising the spatiotemporal power of the optical imaging technique, the optical signals were quantified in several ways. Firstly, it was necessary to examine the baseline patterns of activity, to explore the degree of correspondence between

electrophysiological and optical imaging recordings, and whether the variability between slices justified normalisation procedures. Subsequently, effects of cholinergic drugs on electrophysiological and imaging responses across the stratum radiatum were analysed with comparable methods, in order to determine the suitability of optical imaging for exploring the qualitative and quantitative nature of cholinergic modulation. If results from field recordings and optical imaging were consistent, the superior spatial resolution of the optical imaging technique could be harnessed for a more powerful and detailed analysis of the cholinergic modulation of activity across the CA1 somatodendritic axis.

To allow a primary quantitative comparison of the optical responses across different slices, a 3×20 sampling grid across the CA1 of the hippocampus was used, anchored to the stimulation site in the stratum radiatum. The effects of drugs on the optical response to the first stimulation pulse were normalised to the pre-drug responses, to account for differences in dye loading and allow appropriate comparisons with the normalised fEPSP (see Section 2, and Fig. 2A–F). This was not necessary for the inherently standardised measures of paired-pulse facilitation. This quantification procedure permitted statistical analysis of the spatiotemporal pattern of activity in the hippocampal CA1, which was initially used to examine the baseline profiles of activity in the electrophysiological and optical imaging recordings (Fig. 3).

Analysis of the electrophysiological data prior to drug application in all 72 slices, showed that there was a significant difference between the paired-pulse facilitation recorded at the proximal versus distal electrode during the pre-drug period (1.66 ± 0.02 vs 1.77 ± 0.02, respectively; two-way ANOVA, $F_{(1,\ 111)} = 14.13$, $p < 0.001$) (Fig. 3C). However, there was no significant difference in paired-pulse facilitation between slices used in different drug treatment groups ($F_{(9,\ 111)} = 1.59$, $p = 0.13$), and there was no interaction between drug treatment group and electrode position ($F_{(9,\ 111)} = 0.64$, $p = 0.76$). Therefore, there were no significant systematic differences between the slices used to test for the effects of different drugs.

The optical recording data confirmed the general pattern of activity observed in the electrophysiological data during the period prior to drug application. In the stratum radiatum, there was a significant effect of distance on paired-pulse facilitation (RM ANOVA; $F_{(10.50,\ 640.70)} = 7.43$, $p < 0.001$), while there was no significant effect of drug treatment group and no significant interaction between drug treatment group and distance. The significant effect of distance from the stimulation electrode on the paired-pulse facilitation of the optical signal appeared to be due to a marked reduction in paired-pulse facilitation at sites adjacent to the stimulation electrode (Fig. 3B and C), which is consistent with the electrophysiological recordings.

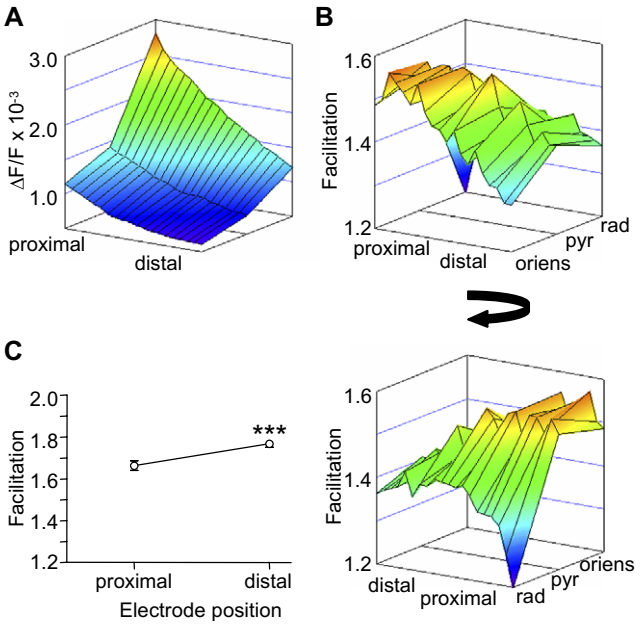

Fig. 3. Pattern of single evoked response and paired-pulse facilitation in CA1 of the hippocampus. Prior to drug application, the responses in all the slices could be averaged to characterise the typical pattern of activation and short-term plasticity in the CA1. (A) The average response to the first stimulation pulse across 72 hippocampal slices. Error bars have been removed for clarity. (B) The average paired-pulse facilitation across the CA1 ($n = 72$). Two views of the 3D graph, shifted by 180°, are provided to allow clear inspection. Error bars have been removed for clarity. (C) The average paired-pulse facilitation of the fEPSP at both proximal and distal field electrodes ($n = 74$). Data are means ± S.E.M. (***$p < 0.001$) (oriens, stratum oriens; pyr, stratum pyramidale; rad, stratum radiatum).

Further analysis of the optical signal across the stratum pyramidale and stratum oriens, revealed that paired-pulse facilitation significantly decreased along the proximodistal axis in both these strata (RM ANOVA; stratum pyramidale, $F_{(9.71,\ 592.32)} = 2.53$, $p < 0.01$; stratum oriens, $F_{(10.62,\ 647.71)} = 3.67$, $p < 0.001$) (Fig. 3B and C). However, there was no significant differences in paired-pulse facilitation between slices used in different drug groups. Therefore, while both field recordings and optical imaging revealed that paired-pulse facilitation varied systematically with distance from the stimulation electrode, there were no significant differences in the pattern of activity between slices prior to drug application, justifying further comparisons in other experimental conditions. To examine whether cholinergic drug treatment had a significant effect on single evoked responses or paired-pulse facilitation, analysis of variance was made across all the different drug groups.

3.3. Cholinergic modulation of single evoked responses in the stratum radiatum of hippocampal CA1

The application of cholinergic drugs had a significant effect on the fEPSP recorded in the CA1 stratum

radiatum (two-way ANOVA; $F_{(9,\ 111)} = 51.72$, $p < 0.001$), which was independent of distance from the stimulation electrode. Post-hoc analysis of the specific means revealed that this cholinergic effect was due to dose-dependent inhibition of activity produced by carbachol application (10 μM carbachol, $p < 0.001$ c.f. control, $p < 0.001$ c.f. 1 μM carbachol; 1 μM carbachol, $p < 0.001$ c.f. control; 0.1 μM carbachol, $p = 1.00$ c.f. control) (Fig. 4A). The effect of 10 μM carbachol was blocked in the presence of 20 μM atropine ($p < 0.001$ c.f. 10 μM carbachol, $p = 1.00$ c.f. control) (Fig. 4A). There were no significant effects of 10 μM nicotine or anti-cholinesterases, 1 μM BW284c51 and 1 μM tacrine, on the fEPSP.

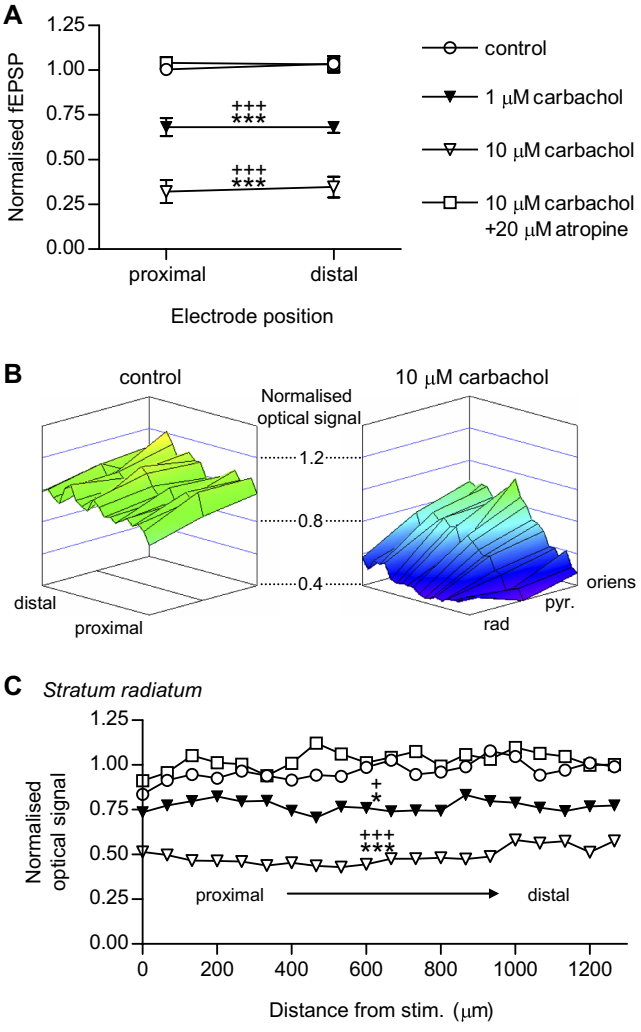

Fig. 4. Muscarinic modulation of the single evoked response in the stratum radiatum. (A) Both 10 μM and 1 μM carbachol inhibited the fEPSP recorded in the stratum radiatum of CA1. The effect of 10 μM carbachol was blocked by 20 μM atropine. (B) Optical data for the average normalised drug effect across the CA1 region for controls and 10 μM carbachol application. Error bars have been removed from the imaging data for clarity. (C) Detailed representation of effects of carbachol in the stratum radiatum shown in (B). In agreement with the recordings of the fEPSP, both 10 μM and 1 μM carbachol inhibited the optical response to the first stimulus in the stratum radiatum. The effect of 10 μM carbachol was blocked by 20 μM atropine. Data are means ± S.E.M. (*$p < 0.05$, ***$p < 0.001$ c.f. control; + $p < 0.05$, +++ $p < 0.001$ c.f. 10 μM carbachol + 20 μM atropine) (oriens, stratum oriens; pyr, stratum pyramidale; rad, stratum radiatum).

Cholinergic modulation of single evoked responses was also apparent in the optical recordings (RM ANOVA; $F_{(9,\ 62)} = 13.66$, $p < 0.001$). Again, this effect was due to a dose-dependent inhibition by carbachol (10 μM carbachol, $p < 0.001$ c.f. control, $p < 0.01$ c.f. 1 μM carbachol; 1 μM carbachol, $p < 0.05$ c.f. control; 0.1 μM carbachol, $p = 1.00$ c.f. control), which was blocked in the presence of 20 μM atropine ($p < 0.001$ c.f. 10 μM carbachol, $p = 1.00$ c.f. control) (Fig. 4C). There were no significant effects of nicotine or anti-cholinesterases, and thus the pattern of results was qualitatively similar to those observed with field recordings, with a slight decrease in sensitivity for detecting drug effects. However, the optical imaging data also revealed that the effects of cholinergic stimulation decreased significantly with distance from the stimulation electrode (RM ANOVA; $F_{(9.12,\ 565.52)} = 4.11$, $p < 0.001$), in a manner which was independent of drug treatment (see Fig. 4B and C). This trend can be observed at the proximal and distal recordings of the fEPSP (Fig. 4A), but recording the optical signal at 20 equidistant points across the CA1 stratum radiatum is clearly more sensitive to this small, but consistent, effect.

3.4. Cholinergic modulation of paired-pulse facilitation in the stratum radiatum of hippocampal CA1

Cholinergic modulation of paired-pulse facilitation was evident in both the electrophysiological (two-way ANOVA; $F_{(9,\ 111)} = 6.79$, $p < 0.001$) and optical imaging recordings in the stratum radiatum (RM ANOVA; $F_{(9,\ 64)} = 2.58$, $p < 0.05$). The paired-pulse facilitation of the fEPSP was significantly augmented by both 10 μM carbachol ($p < 0.001$ c.f. control) and 1 μM carbachol ($p < 0.01$ c.f. control), with the effect of 10 μM carbachol being blocked by 20 μM atropine ($p < 0.001$ c.f. 10 μM carbachol) (Fig. 5A). These changes in paired-pulse facilitation were not as prominent in the optical recordings from the stratum radiatum. Post-hoc analysis revealed that 10 μM carbachol significantly increased the facilitation of the optical response ($p < 0.05$ c.f. control), but 1 μM carbachol had no significant effect (Fig. 5B). Furthermore, the effect of 10 μM carbachol was not completely inhibited by 20 μM atropine ($p = 0.24$ c.f. 10 μM carbachol), although the effect of 10 μM carbachol in the presence of 20 μM atropine was not significantly different to control ($p = 0.99$ c.f. control). There were no significant effects of nicotine or anti-cholinesterases on the paired-pulse facilitation of either the fEPSP or the optical signal.

Overall, in examining the cholinergic modulation of hippocampal CA1 activity, recording the responses in

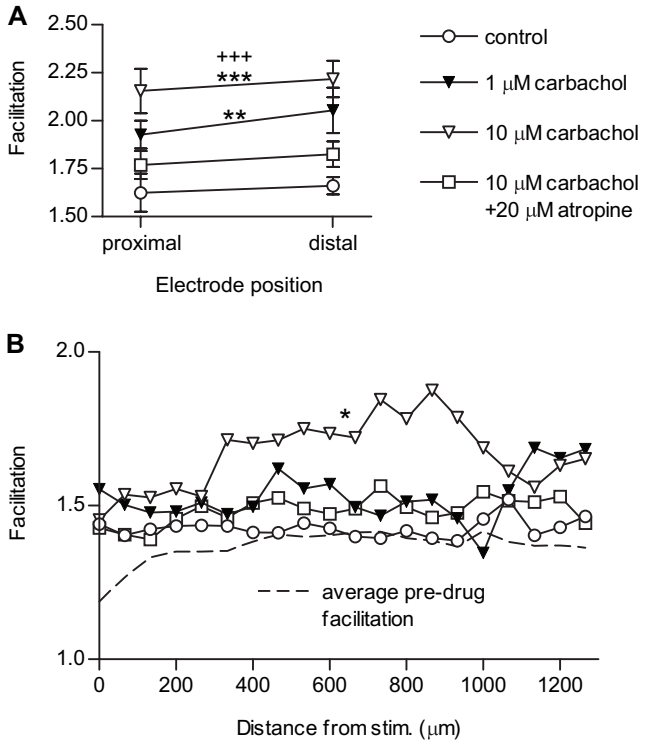

Fig. 5. Muscarinic modulation of paired-pulse facilitation in the stratum radiatum. (A) Paired-pulse facilitation of the fEPSP was significantly increased following the application of carbachol (1 μM and 10 μM), and the effect of 10 μM carbachol was blocked by 20 μM atropine. (B) The paired-pulse facilitation of the optical response was only significantly increased by 10 μM carbachol, and this effect was not directly blocked by 20 μM atropine. However, the co-application of 10 μM carbachol and 20 μM atropine had no significant effect relative to controls. Error bars have been removed from the imaging data for clarity. Data are means ± S.E.M. (*$p < 0.05$, **$p < 0.01$, ***$p < 0.001$ c.f. control; +++ $p < 0.001$ c.f. 10 μM carbachol + 20 μM atropine).

the stratum radiatum to paired-pulse stimulation with field electrodes and optical imaging with VSD provided qualitatively consistent results. The optical imaging technique appeared to be less sensitive for quantitative statistical analysis. However, these results justified using the superior spatial resolution of optical imaging with VSD to explore the cholinergic modulation of responses in the different CA1 layers following input from Schaffer collateral pathway.

3.5. Muscarinic modulation of CA1 activity across the somatodendritic axis

As part of the preliminary quantification of the spatiotemporal activity, normalised drug effects and paired-pulse facilitation were measured across the proximodistal axis of CA1 in both the stratum pyramidale and stratum oriens (see Figs. 2 and 4B). This analysis revealed significant cholinergic modulation of single evoked responses in these layers (RM ANOVA; stratum pyramidale, $F_{(9,\ 62)} = 9.22$, $p < 0.001$; stratum oriens, $F_{(9,\ 62)} = 2.69$, $p < 0.05$), with no significant effects on paired-pulse facilitation. However, as the results from optical imaging appeared consistent with field recordings in the stratum radiatum, a different approach, harnessing more power of the optical imaging technique, was used to explore such modulation across the somatodendritic axis. The actual fractional changes in fluorescence, before and after drug application, were compared at five sites along the somatodendritic axis (stratum oriens, stratum pyramidale, two depths in stratum radiatum, and stratum lacunosum-moleculare), providing more insight into the pattern of activity. These optical signals were collected at a distance from the stimulation electrode at which the signal in the stratum radiatum was at 75–80% of the maximum. The preliminary analysis had shown that cholinergic modulation varied significantly with distance from the stimulation electrode, but there was no significant interaction between distance and drug effects, and so the points from which these signals were collected could be arbitrary. The above criterion provided somatodendritic profiles at 500–800 μm from stimulation electrode, at which responses appeared most invariable over distance (see Figs. 3, 4 and 5B). Such quantification appeared justified, as there were no significant changes in these activity profiles in control experiments.

Examining the effects of 10 μM carbachol on the somatodendritic profile of activity revealed an inhibition of the peak fractional changes in fluorescence (RM ANOVA; $F_{(1,\ 5)} = 41.03$, $p < 0.001$), with a concomitant increase in paired-pulse facilitation ($F_{(1,\ 5)} = 20.97$, $p < 0.01$) (Fig. 6A and B), as would be expected from the previous analysis (see Figs. 4 and 5). However, the effects of this muscarinic agonist were found to vary significantly across the somatodendritic axis (ΔF/F, $F_{(4,\ 20)} = 63.71$, $p < 0.001$; paired-pulse facilitation, $F_{(1,\ 5)} = 10.28$, $p < 0.001$). The inhibitory effect of 10 μM carbachol on single evoked responses was weaker in the perisomatic regions, and there was no significant effect on paired-pulse facilitation in the stratum pyramidale or stratum oriens (see Fig. 6B for detailed p values). The inhibitory effect on single evoked responses was completely blocked in the presence of 20 μM atropine (Fig. 6C). Surprisingly, the application of atropine itself produced a significant increase in paired-pulse facilitation ($F_{(1,\ 7)} = 10.69$, $p < 0.05$), which varied significantly across the somatodendritic axis ($F_{(4,\ 28)} = 3.64$, $p < 0.05$), and was principally confined to perisomatic regions (see Fig. 6B for detailed p values). The application of atropine blocked any further actions of carbachol. These results suggest that muscarinic signalling inhibits the paired-pulse facilitation of signals propagating into the perisomatic regions of CA1. While the baseline paired-pulse facilitation in these regions was relatively high in experiments testing the effects of 10 μM carbachol (see

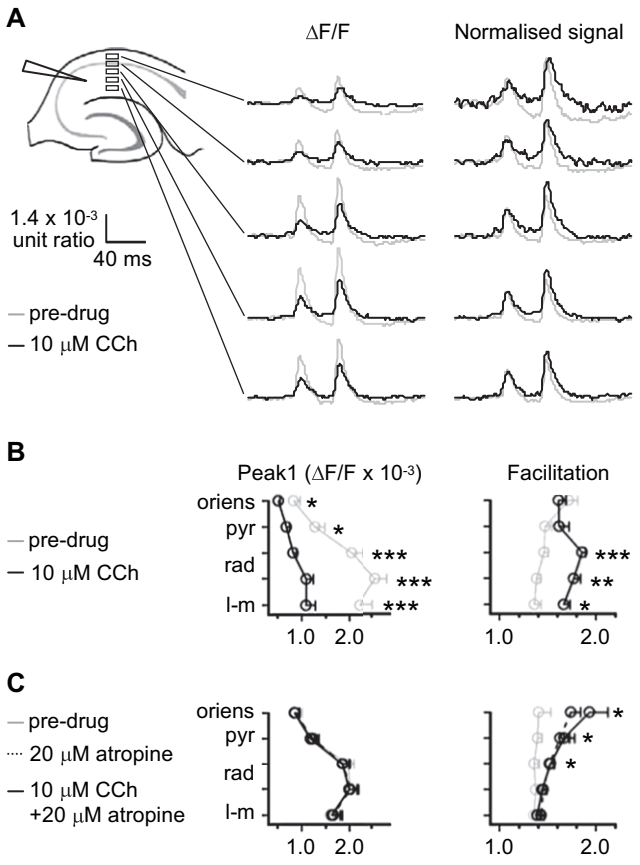

Fig. 6. Muscaranic modulation of activity varies across the somatodendritic axis of hippocampal CA1. (A) Average VSD responses recorded before and after application of 10 μM carbachol ($n = 6$), showing the effect of muscarinic activation on the temporal profile of activity across the CA1, from stratum oriens to stratum lacunosum-moleculare. Optical traces were taken from 7×3 pixel windows positioned at a distance from the stimulation electrode at which the signal in the stratum radiatum had decreased to 75–80% of maximum (500–800 μm). The pattern of activity is shown as both the fractional change in fluorescence and the normalised signal, where traces have been scaled so the single evoked responses are of equal amplitude. Traces were temporally aligned on the stimulation time, rather than the time of peak. (B) Quantification of the effects of 10 μM carbachol on the peak fractional change in fluorescence and paired-pulse facilitation. Both of these measures were independent of time to peak. The application of 10 μM carbachol inhibited single evoked responses across the somatodendritic axis, with effects weaker in perisomatic regions. The inhibition of responses in perisomatic regions was not accompanied by increases in paired-pulse facilitation. (C) The inhibition of single evoked responses by 10 μM carbachol was completely blocked by 20 μM atropine. Atropine alone produced a selective increase in paired-pulse facilitation in perisomatic regions, but blocked any further effects of carbachol. Data are means ± S.E.M. (*$p < 0.05$, **$p < 0.01$, ***$p < 0.001$ c.f. pre-drug) (oriens, stratum oriens; pyr, stratum pyramidale; rad, stratum radiatum; l-m, stratum lacunosum-moleculare).

Fig. 6A and B), the same pattern of effects was observed with 1 μM carbachol (data not shown) while atropine had the opposite effect, and thus the somatodendritic variation in muscarinic modulation appeared independent of the original activity profile.

3.6. Nicotinic modulation of CA1 activity across the somatodendritic axis

Nicotine was found earlier to have no effects on activity recorded in the stratum radiatum. Indeed, when examining nicotinic modulation of the somatodendritic profile of activity, 10 μM nicotine was found to have no significant effects on single evoked responses (Fig. 7). In contrast, there was a significant increase in paired-pulse facilitation (RM ANOVA; $F_{(1,\ 4)} = 23.49$, $p < 0.01$), that was selectively observed in perisomatic regions ($F_{(1.98,\ 7.93)} = 4.91$, $p < 0.05$) (see Fig. 7B for detailed p values). This effect was at least partially blocked by both the α7 nAChR antagonist, 50 nM bungarotoxin ($F_{(1,\ 5)} = 3.43$, $p = 0.12$), and the non-α7 nAChR antagonist, 25 μM mecamylamine ($F_{(1,\ 5)} = 4.73$, $p = 0.08$). Neither of these antagonists had effects when applied alone, and therefore the nicotinic modulation of paired-pulse facilitation of signals propagating into perisomatic regions appeared to be due to activation of both α7 and non-α7 nAChR.

3.7. Modulation of CA1 activity across the somatodendritic axis by endogenous cholinergic transmission

Activation of mAChR and nAChR appeared to have very different effects on the somatodendritic profile of activity. To provide insight into the net modulation

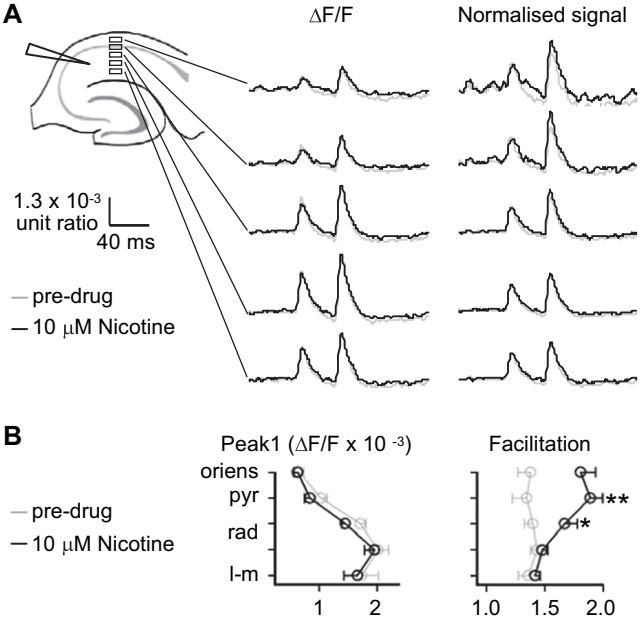

Fig. 7. Nicotinic receptor activation selectively enhances the facilitation of perisomatic responses. (A) Average VSD responses recorded before and after application of 10 μM nicotine ($n = 5$). (B) Nicotine had no significant effect on the response to single stimuli, but selectively increased the paired-pulse facilitation towards perisomatic regions of CA1. Data are means ± S.E.M. (*$p < 0.05$, **$p < 0.01$ c.f. pre-drug) (oriens, stratum oriens; pyr, stratum pyramidale; rad, stratum radiatum; l-m, stratum lacunosum-moleculare).

produced by endogenous acetylcholine release, the effects of anti-cholinesterases were explored. In the original analysis comparing electrophysiological and optical imaging recordings in the stratum radiatum, no significant effects of anti-cholinesterases were observed. However, examining the somatodendritic profile of activity revealed that the anti-cholinesterase, 1 μM BW284c51, significantly inhibited single evoked responses (RM ANOVA; $F_{(1,\ 7)} = 35.12$, $p < 0.001$). This inhibition was small, but consistent across all layers of the CA1 (mean $\Delta F/F$ across all layers reduced from $1.7 \pm 0.2 \times 10^{-3}$ to $1.4 \pm 0.1 \times 10^{-3}$; data not shown). This inhibition of evoked responses was accompanied by a significant increase in paired-pulse facilitation ($F_{(1,\ 7)} = 10.82$, $p < 0.05$), which was also consistent across the somatodendritic axis. This might suggest that endogenous cholinergic signalling, by acting via both mAChR and nAChR, has a relatively uniform effect on evoked responses across different layers of CA1. However, another anti-cholinesterase, 1 μM tacrine, had no significant effects on the somatodendritic profile of activity, suggesting that the effects of BW284c51 might not have been entirely due to inhibition of the enzymatic activity of cholinesterases.

3.8. Cholinergic modulation of the response to tetanic stimulation and LTP

In addition to examining the cholinergic modulation of hippocampal activity, another aim of this study was to examine how cholinergic drugs modulate the pattern of long-term changes in synaptic plasticity. This was addressed by inducing LTP with a tetanus of high-frequency stimulation (100 Hz, 1 s), following 30 min for the equilibration of drug effects (Fig. 8A). In the majority of experiments, the optical response to tetanization was recorded, affording the analysis of cholinergic modulation of the response to high-frequency afferent stimulation.

It was found that cholinergic drug application had a significant effect on the optically recorded response to high-frequency stimulation in the stratum radiatum (RM ANOVA; $F_{(9,\ 54)} = 4.92$, $p < 0.001$). Post-hoc analysis of the between-subjects effects revealed that this was due to the significant increase in the optical response produced by 10 μM carbachol ($p < 0.001$ c.f. control) (see Fig. 8B and C), which was blocked by 20 μM atropine ($p < 0.001$ c.f. 10 μM carbachol). This enhancement of the response to high-frequency stimulation was significantly greater at sites closer to the stimulation electrode ($F_{(4.96,\ 267.64)} = 1.78$, $p < 0.01$; see Fig. 8C for detailed p values), and therefore appeared to be explained by a interaction between the greater activation at proximal sites and the effects of carbachol on facilitation (see Figs. 5B and 8B).

The cholinergic modulation of the optical response to high-frequency activation was different in the other two layers of the hippocampus. Across the proximodistal extent of stratum pyramidale, there was a significant effect of drug treatment (RM ANOVA; $F_{(9,\ 54)} = 3.47$, $p < 0.01$), predominantly due to the significant attenuation of the tetanization response produced by 0.1 μM carbachol ($p < 0.05$ c.f. control) (data not shown). This effect was significantly different from the effect of 10 μM carbachol ($p < 0.01$ c.f. 10 μM carbachol), which produced an insignificant augmentation of the response at proximal sites ($p = 0.90$ c.f. control). Across the proximodistal extent of stratum oriens, there was again a significant effect of drug treatment ($F_{(9,\ 54)} = 2.85$, $p < 0.01$), but post-hoc analysis revealed no significant effects of specific drugs. The effects appeared similar to those in the stratum pyramidale, with 0.1 μM carbachol producing an inhibition of the optical response which approached significance ($p = 0.13$ c.f. control), and 10 μM carbachol producing an insignificant increase in the response at proximal sites ($p = 0.93$ c.f. control) (data not shown). However, while these dose-dependent effects of carbachol were potentially interesting, a detailed analysis of the responses to tetanic stimulation across the somatodendritic axis depended on such cholinergic modulation having a significant effect on the pattern of LTP.

The LTP induced by high-frequency afferent stimulation was measured >50 min following tetanization. It was found that cholinergic drug treatment had no significant effect on LTP of either the fEPSP or the optically recorded responses in stratum radiatum, stratum pyramidale and stratum oriens (see Fig. 8D and E). There was a significant effect of distance on the optically recorded LTP in the stratum radiatum (RM ANOVA; $F_{(10.29,\ 637.79)} = 3.59$, $p < 0.001$) and stratum pyramidale ($F_{(13.26,\ 822.37)} = 1.76$, $p < 0.05$), which appeared to be predominantly due to an increased LTP at proximal perisomatic and distal sites (Fig. 8D and E). However, the variation of LTP across the stratum radiatum was not apparent in the electrophysiological data.

The induction of LTP also appeared to have little effect on the pattern of paired-pulse facilitation. Following LTP induction, paired-pulse facilitation of the fEPSP was significantly greater at proximal versus distal sites (1.70 ± 0.03 vs 1.81 ± 0.02 respectively), which was similar to that observed in the analysis of pre-drug and drug application periods. Slices that had been treated with carbachol continued to express a higher paired-pulse facilitation following LTP induction (10 μM carbachol, $p < 0.001$ c.f. control; 1 μM carbachol groups, $p < 0.05$ c.f. control), which was not observed in the presence of 20 μM atropine ($p < 0.001$ c.f. 10 μM carbachol). This pattern was similar to that observed in the drug application period, suggesting that

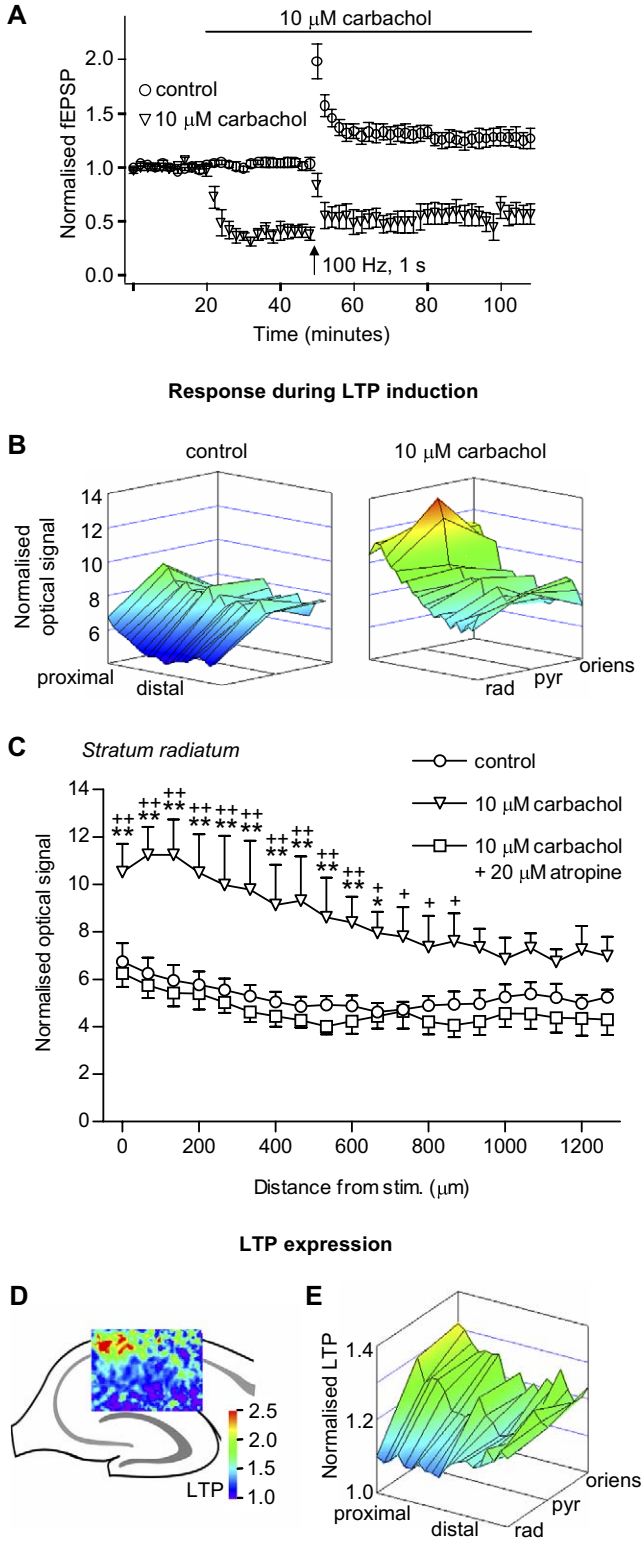

Fig. 8. Cholinergic modulation of LTP. (A) The average time course of LTP of the fEPSP in control experiments and in the presence of 10 μM carbachol. The VSD responses were recorded during tetanization (100 Hz, 1 s), to examine the response during LTP induction, and >50 min after induction, to examine the pattern of activity following LTP expression. In both cases stable LTP was recorded for over 1 h. (B) The average normalised optical response to 100 Hz stimulation for 1 s across the CA1 region for control experiments and in the presence of 10 μM carbachol. Error bars have been removed for clarity. (C) Details of the response in stratum radiatum. The presence of 10 μM carbachol significantly increased the response to tetanus stimulation selectively at sites proximal to the stimulation electrode, and this effect was blocked by 20 μM atropine. (D) Pseudo-colour representation of the spatial pattern of LTP measured in a representative slice using optical imaging with VSD. (E) No significant effect of cholinergic drug treatment on LTP could be detected. The 3D graph depicts the average LTP measured across all slices ($n = 72$). Error bars have been removed for clarity. Data are means ± S.E.M. (*$p < 0.05$, **$p < 0.01$ c.f. control; + $p < 0.05$, ++ $p < 0.01$ c.f. 10 μM carbachol + 20 μM atropine) (oriens, stratum oriens; pyr, stratum pyramidale; rad, stratum radiatum).

the cholinergic modulation of the CA1 activity had little interaction with the induction of LTP. However, the effects of carbachol on paired-pulse facilitation of the fEPSP did appear to be reduced following LTP induction, and this could explain why no significant effects of drug treatment were found for the paired-pulse facilitation of the optical signal in the stratum radiatum following LTP induction (RM ANOVA; $F_{(9, 61)} = 1.70$, $p = 0.11$). As no significant cholinergic modulation of LTP could be observed, and the responses recorded using field electrodes and optical imaging no longer appeared analogous, the detailed somatodendritic profiles of activity during tetanic stimulation and following LTP induction were not analysed.

4. Discussion

4.1. The source of the optical signal

The technique of optical imaging with VSDs in vitro clearly offers a powerful tool to study hippocampal network activity, but it is important to understand the origin of the optical signal recorded. It is possible for the optical recording to be contaminated with intrinsic signals (Holthoff and Witte, 1996; Cerne and Haglund, 2002) and/or signals from non-specifically stained elements, such as glia (Yuste et al., 1997; Kojima et al., 1999). However, these signals develop slowly after the onset of activity, while the optical signals recorded in this study showed no slow response, and were back to baseline levels within 100 ms following the first stimulation (see Fig. 1). The neuronal signals themselves can arise from heterogeneous elements, including pre-synaptic terminals, dendrites and somata. Indeed, in neocortical slices, pre-synaptic activity can contribute up 65% of the optical signal (Yuste et al., 1997). However, some of the authors have already shown that pharmacological blockade of glutamatergic transmission inhibits the majority of the optical signal in our preparation (Tominaga et al., 2000). As the number of interneurons is relatively small (Freund and Buzsaki, 1996), this post-synaptic optical signal predominantly reflects voltage changes in CA1 pyramidal cells. This result is consistent with the correlation between the optical signal in the stratum radiatum and the fEPSP in this study (see Fig. 1C), as the peak in the extracellular current, where one would expect the maximum change in post-synaptic voltage, coincided with the maximum change in the optical signal. The advantage of optical imaging with VSDs in monitoring network activity is that the post-synaptic voltage changes can be recorded across the extent of the dendritic tree and over the breadth of the CA1.

4.2. Quantitative analysis of spatiotemporal activity

Examining the source of the optical signal reveals the problems inherent in quantitative analysis using optical imaging with VSDs. Indeed, in cortical preparations, this technique has predominantly been used to track the spread of activity between brain regions and to examine functional connectivity (Iijima et al., 1996; Shoham et al., 1999). There have been very few attempts at systems pharmacology, involving quantitative comparisons of drug actions. In some cases, normalisation and sampling techniques have been used to allow averaging over different experiments (Kimura et al., 1999; Haupt, 2000), but these results have not been analysed statistically. Such statistical analysis has largely been confined to single measurements of the spread of activation (Laaris et al., 2000), which may entail the loss of the spatial information. The aim of this project was the statistical evaluation of cholinergic modulation in 2-dimensions across the entire hippocampal CA1 region, and therefore it was necessary to re-evaluate the problems of quantitative analysis and develop a new approach.

The initial phase of analysis was designed to provide insight into how the patterns of activity recorded across CA1 varied between slices, and thus whether it was legitimate to explore the cholinergic modulation over the CA1 network. Furthermore, it was necessary to determine whether the effects of cholinergic modulation observed using optical imaging and traditional field recordings were consistent. To enable such quantitative comparisons across different slices, the fractional changes in fluorescence obtained from optical imaging were normalised, making these measures independent of variations in dye loading, individual anatomical differences between slices and the non-uniform Schaffer collateral projection in the CA1 (Amaral and Witter, 1989). Mapping of such activity patterns between different slices was achieved by using a sampling method, based on the technique employed by Kimura et al. (1999). This sampling method was extended from one dimension, to include the stratum radiatum, stratum pyramidale and stratum oriens (see Fig. 2). The results of these sampling and normalisation procedures demonstrated that there were no significant differences in the pattern of paired-pulse facilitation of the optical response between different slices (see Fig. 3). Moreover, optical imaging with VSD revealed qualitatively the same cholinergic modulation of activity as electrophysiological recordings, although analysis of the imaging data were less sensitive to quantitative changes (Figs. 4 and 5). With detailed information regarding the proximodistal variations in activity patterns and drug effects, and the reliability of the optical signal, it was then valid to exploit the resolution of the optical imaging technique to examine cholinergic modulation

across the somatodendritic axis within individual slices. In this analysis the actual fractional changes in fluorescence of the VSD could be compared, with the statistical design accounting for differences between slices. While the validity of this approach depended on the initial analysis, it proved more powerful in revealing the intricacies of cholinergic modulation (see Figs. 6 and 7).

4.3. Muscarinic modulation of hippocampal activity

Muscarinic receptors can influence hippocampal activity by modulating neurotransmitter release and a variety of ionic conductances, but it is not clear how a balance between these heterogeneous actions develops, or how these interactions manifest at the network level. The characteristic lamina-specific distribution of mAChR subtypes could offer some insight into their functional role in the network (Levey et al., 1995), but such features of hippocampal physiology have not been fully explored. The characteristics of muscarinic modulation of hippocampal activity were explored in this study through the application of three different concentrations of the non-selective mAChR agonist, carbachol (0.1 μM, 1 μM and 10 μM), which can produce strikingly different effects on hippocampal network activity (Fellous and Sejnowski, 2000).

The application of carbachol (1 μM and 10 μM) produced a dose-dependent inhibition of the evoked response in the stratum radiatum, whilst 0.1 μM carbachol had no significant effect. The effect of 10 μM carbachol was blocked by 20 μM atropine, and was not mimicked by nicotine application, suggesting a selective action of carbachol at mAChR. The inhibitory effect appeared relatively uniform across the stratum radiatum, although there was a small but significant trend for decreased effects at more distal sites, probably reflecting the degree of activation (Fig. 4). This is consistent with the relatively homogeneous distribution of mAChR along this axis of the CA1 (Levey et al., 1995). The inhibition of the evoked response in the stratum radiatum was accompanied by an increase in paired-pulse facilitation, suggesting that the effect was at least partially pre-synaptic in origin (Fig. 5). Although no subtype selective antagonists were used, such a pre-synaptic effect was most probably mediated by the M_2 receptor (Rouse et al., 2000).

The muscarinic suppression of single evoked responses was evident across the somatodendritic axis of CA1, but was less prominent in perisomatic regions (Fig. 6). This pattern appeared to reflect the degree of activation, with perisomatic signals already attenuated during propagation along the somatodendritic axis. More interestingly, the suppression of evoked responses at perisomatic sites was not accompanied by increases in paired-pulse facilitation (Fig. 6B). It is difficult to infer the cellular mechanisms underlying this effect, as mAChR activation produces an array of effects on pyramidal cells (Benson et al., 1988) and interneurons (McQuiston and Madison, 1999a,b), which could interact in complex ways (for example see Martin and Alger, 1999). Examining the time course of the responses to paired-pulse stimulation suggested that mAChR activation reduced the speed of membrane repolarisation across the somatodendritic axis (see Fig. 6A). This could be due to muscarinic inhibition of post-synaptic potassium currents, such as I_M or a potassium leak current (Benson et al., 1988; Storm, 1990), or a reduction in phasic inhibition (Behrends and ten Bruggencate, 1993), but such effects would be expected to increase the response to a second stimulus. Therefore, an additional shunting mechanism appeared to prevent facilitated responses in the apical dendrites propagating to perisomatic sites. This mechanism appeared to be modulated by a constitutively active muscarinic signalling pathway as atropine, a mAChR antagonist/inverse agonist, had no significant effect on single evoked responses while selectively increasing paired-pulse facilitation at perisomatic sites, and completely blocked further effects of carbachol (Fig. 6C). One mechanism that could explain this effect is the modulation of an inwardly rectifying potassium conductance by mAChR located post-synaptically on pyramidal neurons (Seeger and Alzheimer, 2001). Due to the voltage-dependency of this conductance, one might expect strong and/or high-frequency stimulation would overcome such a shunting mechanism. Consistent with this hypothesis, the application of carbachol increased paired-pulse facilitation, and the response to tetanic stimulation, in perisomatic regions proximal to the stimulation electrode (data not shown).

4.4. Nicotinic modulation of hippocampal activity

The application of nicotine had no significant effect on single evoked responses, but selectively increased paired-pulse facilitation towards perisomatic sites (Fig. 7). This effect was partially blocked by both 50 nM bungarotoxin and 25 μM mecamylamine, and thus appeared to be due to activation of both α7 and non-α7 nAChR, respectively. Hippocampal nAChR are predominantly located on interneurons (Sudweeks and Yakel, 2000), and so these effects may represent a reduction in perisomatic feedback inhibition. Although nicotine was not found to modulate LTP in this study, such a selective nicotinic facilitation of perisomatic responses to repetitive stimulation could explain why nicotine has been shown to lower the threshold for the induction of synaptic plasticity, without affecting basal synaptic transmission (Fuji et al., 1999; Mann and Greenfield, 2003).

4.5. The effects of anti-cholinesterases on hippocampal activity

As activation of mAChR and nAChR produced different effects on hippocampal activity, it was of interest to explore the effects of endogenous cholinergic transmission by blocking cholinesterase activity. Both anti-cholinesterases tested, 1 μM BW284c51 and 1 μM tacrine, produced a small and insignificant inhibition of the fEPSP and normalised optical response recorded across the proximodistal extent of the stratum radiatum. Analysing the effects of anti-cholinesterases on the somatodendritic profile of activity, which consistently proved statistically more sensitive than the proximodistal analysis, suggested that BW284c51 produced a significant inhibition of responses across all layers of CA1 that was accompanied by an increase in paired-pulse facilitation. This is consistent with an additive effect of mAChR and nAChR activation produced by endogenous acetylcholine release. However, tacrine did not significantly change the somatodendritic activity profile, despite having similar anti-cholinesterase activity. Therefore, the effects of BW284c51 may have been due to non-specific actions or a blockade of putative non-enzymatic functions of AChE (Jones et al., 1995; Bataille et al., 1998; Soreq and Seidman, 2001). Indeed, the minor effects of tacrine and AChR antagonists suggest that endogenous release of acetylcholine was low in this slice preparation, although some muscarinic signalling pathways may have been constitutively active (see above).

4.6. Examining LTP using optical imaging with VSD

The various effects of cholinergic signalling on CA1 activity might be expected to modulate the induction and expression of synaptic plasticity. Such cholinergic modulation was explored by recording the response to tetanic stimulation and the pattern of activity following LTP induction (Fig. 8). Application of 10 μM carbachol was found to increase the response to the tetanus in the stratum radiatum, with this effect significantly greater at proximal versus distal sites, probably reflecting the degree of afferent activity (Fig. 8B and C). There were also some contrasting effects of different concentrations of carbachol on the response to tetanic stimulation in the perisomatic regions of CA1, which might suggest that different transduction pathways predominate at different levels of mAChR activation (data not shown). However, these effects were not analysed in detail, as there was no subsequent effect on the pattern of LTP recorded (Fig. 8D).

The failure to reveal significant cholinergic modulation of LTP is surprising given the apparent importance of the cholinergic signalling to hippocampal synaptic plasticity in vivo (see Rasmusson, 2000 for review). However, several experiments have demonstrated only minor effects of cholinergic drugs on LTP in the hippocampal CA1 in vitro (Segal and Auerbach, 1997; Shimoshige et al., 1997; Yun et al., 2000; Ye et al., 2001; but see Auerbach and Segal, 1994, 1996), and the experimental and analytical design used here may not have been sensitive to such small changes. Indeed, the most notable feature was the low amplitude of LTP recorded with optical imaging (Fig. 8D and E). The optical imaging measurements of LTP were monitored ~2 h following the start of the experiment and may have been reduced by wash-out of the dye and photobleaching. As each slice received the same light exposure and the optical signals were normalised, these results remained comparable, but the resulting reduction in the signal amplitude made assessing changes in the degree of LTP expression difficult. Therefore, while optical imaging with VSDs has previously been used successfully for long-term recording of LTP (Mochida et al., 2001; Hosokawa et al., 2003), it appears that the experimental paradigm described here may not be primarily suited to the quantitative analysis of drug effects on such long-term plastic changes.

5. Concluding remarks

This study demonstrates that optical imaging with VSD can be used reliably for quantitative analysis of the cholinergic modulation of hippocampal activity. Given the good correlation between the effects observed with recordings of VSD and electrophysiological signals, the greater spatial resolution of optical imaging was used to explore the cholinergic modulation of the spatiotemporal pattern of activity across the CA1 network. The effects of cholinergic drugs were found to vary across the proximodistal extent of CA1, probably reflecting the degree of activation. This could be important from a practical point of view, as it implies that the observed effects of cholinergic drugs with single electrode recordings might be dependent on the recording site. More interestingly, the effects of muscarinic and nicotinic receptor activation were found to have differential effects on responses across the somatodendritic axis of CA1. The activation of mAChR was found to inhibit the response to single stimuli and increase paired-pulse facilitation, while preventing the facilitated response to repetitive stimulation propagating to perisomatic regions. In contrast, nAChR activation had no effect on responses to single stimuli, but selectively increased the perisomatic response to repetitive stimuli. These results might provide insight into how cholinergic signalling modulates the somatodendritic processing of inputs to the hippocampal CA1 network.

Acknowledgements

E.O.M. was supported by the Schorstein Research Fellowship, Oxford University Medical School, the REES programme and RIKEN summer programme. We would like to thank Dr Chris Price for his very helpful comments on the manuscript.

References

Amaral, D.G., Witter, M.P., 1989. The 3-dimensional organization of the hippocampal-formation – a review of anatomical data. Neuroscience 31, 571–591.

Auerbach, J.M., Segal, M., 1994. A novel cholinergic induction of long-term potentiation in rat hippocampus. Journal of Neurophysiology 72, 2034–2040.

Auerbach, J.M., Segal, M., 1996. Muscarinic receptors mediating depression and long-term potentiation in rat hippocampus. Journal of Physiology 492, 479–493.

Bataille, S., Portalier, P., Coulon, P., Ternaux, J.P., 1998. Influence of acetylcholinesterase on embryonic spinal rat motoneurones growth in culture: a quantitative morphometric study. European Journal of Neuroscience 10, 560–572.

Behrends, J.C., ten Bruggencate, G., 1993. Cholinergic modulation of synaptic inhibition in the guinea pig hippocampus in vitro: excitation of GABAergic interneurons and inhibition of GABA-release. Journal of Neurophysiology 69, 626–629.

Benson, D.M., Blitzer, R.D., Landau, E.M., 1988. An analysis of the depolarization produced in guinea-pig hippocampus by cholinergic receptor stimulation. Journal of Physiology 404, 479–496.

Cerne, R., Haglund, M.M., 2002. Electrophysiological correlates to the intrinsic optical signal in the rat neocortical slice. Neuroscience Letters 317, 147–150.

Colino, A., Halliwell, J.V., 1993. Carbachol potentiates Q-current and activates a calcium-dependent nonspecific conductance in rat hippocampus in-vitro. European Journal of Neuroscience 5, 1198–1209.

Descarries, L., Gisiger, V., Steriade, M., 1997. Diffuse transmission by acetylcholine in the CNS. Progress in Neurobiology 53, 603–625.

Dutar, P., Bassant, M.H., Senut, M.C., Lamour, Y., 1995. The septohippocampal pathway: structure and function of a central cholinergic system. Physiological Reviews 75, 393–427.

Dvorak-Carbone, H., Schuman, E.M., 1999. Patterned activity in stratum lacunosum moleculare inhibits CA1 pyramidal neuron firing. Journal of Neurophysiology 82, 3213–3222.

Fellous, J.M., Sejnowski, T.J., 2000. Cholinergic induction of oscillations in the hippocampal slice in the slow (0.5–2 Hz), theta (5–12 Hz), and gamma (35–70 Hz) bands. Hippocampus 10, 187–197.

Fitzpatrick, D., 2000. Cortical imaging: capturing the moment. Current Biology 10, R187–R190.

Francis, P.T., Palmer, A.M., Snape, M., Wilcock, G.K., 1999. The cholinergic hypothesis of Alzheimer's disease: a review of progress. Journal of Neurology, Neurosurgery & Psychiatry 66, 137–147.

Freund, T.F., Buzsaki, G., 1996. Interneurons of the hippocampus. Hippocampus 6, 347–470.

Fuji, S., Ji, Z., Morita, N., Sumikawa, K., 1999. Acute and chronic nicotine exposure differentially facilitate the induction of LTP. Brain Research 846, 137–143.

Giacobini, E., 1998. Invited review: cholinesterase inhibitors for Alzheimer's disease therapy: from tacrine to future applications. Neurochemistry International 32, 413–419.

Grinvald, A., Manker, A., Segal, M., 1982. Visualization of the spread of electrical activity in rat hippocampal slices by voltage-sensitive optical probes. Journal of Physiology 333, 269–291.

Haupt, S.S., 2000. Optical recording of spatiotemporal activation of rat somatosensory and visual cortex in vitro. Neuroscience Letters 287, 29–32.

Holthoff, K., Witte, O.W., 1996. Intrinsic optical signals in rat neocortical slices measured with near-infrared dark-field microscopy reveal changes in extracellular space. Journal of Neuroscience 16, 2740–2749.

Hosokawa, T., Ohta, M., Saito, T., Fine, A., 2003. Imaging spatiotemporal patterns of long-term potentiation in mouse hippocampus. Philosophical Transactions of the Royal Society London B Biological Sciences 358, 689–693.

Iijima, T., Witter, M.P., Ichikawa, M., Tominaga, T., Kajiwara, R., Matsumoto, G., 1996. Entorhinal–hippocampal interactions revealed by real-time imaging. Science 272, 1176–1179.

Jones, S.A., Holmes, C., Budd, T.C., Greenfield, S.A., 1995. The effect of acetylcholinesterase on outgrowth of dopaminergic neurons in organotypic slice culture of rat mid-brain. Cell and Tissue Research 279, 323–330.

Kimura, F., Fukuda, M., Tsumoto, T., 1999. Acetylcholine suppresses the spread of excitation in the visual cortex revealed by optical recording: possible differential effect depending on the source of input. European Journal of Neuroscience 11, 3597–3609.

Kojima, S., Nakamura, T., Nidaira, T., Nakamura, K., Ooashi, N., Ito, E., Watase, K., Tanaka, K., Wada, K., Kudo, Y., Miyakawa, H., 1999. Optical detection of synaptically induced glutamate transport in hippocampal slices. Journal of Neuroscience 19, 2580–2588.

Laaris, N., Carlson, G.C., Keller, A., 2000. Thalamic-evoked synaptic interactions in barrel cortex revealed by optical imaging. Journal of Neuroscience 20, 1529–1537.

Levey, A.I., Edmunds, S.M., Koliatsos, V., Wiley, R.G., Heilman, C.J., 1995. Expression of M1–M4 muscarinic acetylcholine-receptor proteins in rat hippocampus and regulation by cholinergic innervation. Journal of Neuroscience 15, 4077–4092.

Mann, E.O., Greenfield, S.A., 2003. Novel modulatory mechanisms revealed by the sustained application of nicotine in the guinea-pig hippocampus in vitro. Journal of Physiology 551, 539–550.

Martin, L.A., Alger, B.E., 1999. Muscarinic facilitation of the occurrence of depolarization-induced suppression of inhibition in rat hippocampus. Neuroscience 92, 61–71.

McQuiston, A.R., Madison, D.V., 1999a. Muscarinic receptor activity has multiple effects on the resting membrane potentials of CA1 hippocampal interneurons. Journal of Neuroscience 19, 5693–5702.

McQuiston, A.R., Madison, D.V., 1999b. Muscarinic receptor activity induces an afterdepolarization in a subpopulation of hippocampal CA1 interneurons. Journal of Neuroscience 19, 5703–5710.

McQuiston, A.R., Madison, D.V., 1999c. Nicotinic receptor activation excites distinct subtypes of interneurons in the rat hippocampus. Journal of Neuroscience 19, 2887–2896.

Mochida, H., Sato, K., Sasaki, S., Yazawa, I., Kamino, K., Momose-Sato, Y., 2001. Effects of anisomycin on LTP in the hippocampal CAI: long-term analysis using optical recording. Neuroreport 12, 987–991.

Peterlin, Z.A., Kozloski, J., Mao, B.Q., Tsiola, A., Yuste, R., 2000. Optical probing of neuronal circuits with calcium indicators. Proceedings of the National Academy of Sciences USA 97, 3619–3624.

Rasmusson, D.D., 2000. The role of acetylcholine in cortical synaptic plasticity. Behavioural Brain Research 115, 205–218.

Ratzlaff, E.H., Grinvald, A., 1991. A tandem-lens epifluorescence macroscope: hundred-fold brightness advantage for wide-field imaging. Journal of Neuroscience Methods 36, 127–137.

Rouse, S.T., Edmunds, S.M., Yi, H., Gilmor, M.L., Levey, A.I., 2000. Localization of M-2 muscarinic acetylcholine receptor protein in

cholinergic and non-cholinergic terminals in rat hippocampus. Neuroscience Letters 284, 182–186.

Seeger, T., Alzheimer, C., 2001. Muscarinic activation of inwardly rectifying K+ conductance reduces EPSPs in rat hippocampal CA1 pyramidal cells. Journal of Physiology 535, 383–396.

Segal, M., Auerbach, J.M., 1997. Muscarinic receptors involved in hippocampal plasticity. Life Sciences 60, 1085–1091.

Shimoshige, Y., Maeda, T., Kaneko, S., Akaike, A., Satoh, M., 1997. Involvement of M(2) receptor in an enhancement of long-term potentiation by carbachol in Schaffer collateral-CA1 synapses of hippocampal slices. Neuroscience Research 27, 175–180.

Shoham, D., Glaser, D.E., Arieli, A., Kenet, T., Wijnbergen, C., Toledo, Y., Hildesheim, R., Grinvald, A., 1999. Imaging cortical dynamics at high spatial and temporal resolution with novel blue voltage-sensitive dyes. Neuron 24, 791–802.

Soreq, H., Seidman, S., 2001. Acetylcholinesterase – new roles for an old actor. Nature Reviews in Neuroscience 2, 294–302.

Squire, L.R., 1992. Memory and the hippocampus – a synthesis from findings with rats, monkeys, and humans. Psychological Review 99, 195–231.

Storm, J.F., 1990. Potassium currents in hippocampal pyramidal cells. Progress in Brain Research 83, 161–187.

Sudweeks, S.N., Yakel, J.L., 2000. Functional and molecular characterization of neuronal nicotinic ACh receptors in rat CA1hippocampal neurons. Journal of Physiology 527, 515–528.

Tominaga, T., Tominaga, Y., Yamada, H., Matsumoto, G., Ichikawa, M., 2000. Quantification of optical signals with electrophysiological signals in neural activities of Di-4-ANEPPS stained rat hippocampal slices. Journal of Neuroscience Methods 102, 11–23.

Ye, L., Qi, J.S., Qiao, J.T., 2001. Long-term potentiation in hippocampus of rats is enhanced by endogenous acetylcholine in a way that is independent of *N*-methyl-D-aspartate receptors. Neuroscience Letters 300, 145–148.

Yun, S.H., Cheong, M.Y., Mook-Jung, I., Huh, K., Lee, C., Jung, M.W., 2000. Cholinergic modulation of synaptic transmission and plasticity in entorhinal cortex and hippocampus of the rat. Neuroscience 97, 671–676.

Yuste, R., Tank, D.W., Kleinfeld, D., 1997. Functional study of the rat cortical microcircuitry with voltage-sensitive dye imaging of neocortical slices. Cerebral Cortex 7, 546–558.

Zochowski, M., Wachowiak, M., Falk, C.X., Cohen, L.B., Lam, Y.W., Antic, S., Zecevic, D., 2000. Concepts in imaging and microscopy – imaging membrane potential with voltage-sensitive dyes. Biological Bulletin 198, 1–21.